Determination of compositeness of the $\Lambda(1405)$ resonance from its radiative decay

T. Sekihara[1,*] and S. Kumano[1,2]

[1]*KEK Theory Center, Institute of Particle and Nuclear Studies, High Energy Accelerator Research Organization (KEK), 1-1 Oho, Tsukuba, Ibaraki 305-0801, Japan*

[2]*J-PARC Branch, KEK Theory Center, Institute of Particle and Nuclear Studies, High Energy Accelerator Research Organization (KEK), 203-1 Shirakata, Tokai, Ibaraki 319-1106, Japan*

(Received 22 November 2013; published 18 February 2014)

The radiative decay of $\Lambda(1405)$ is investigated from the viewpoint of compositeness, which corresponds to the amount of two-body states composing resonances as well as bound states. For a $\bar{K}N(I=0)$ bound state without couplings to other channels, we establish a relation between the radiative decay width and the compositeness. Especially the radiative decay width of the bound state is proportional to the compositeness. Applying the formulation to $\Lambda(1405)$, we observe that the decay to $\Lambda\gamma$ is dominated by the K^-p component inside $\Lambda(1405)$, because in this decay $\pi^+\Sigma^-$ and $\pi^-\Sigma^+$ strongly cancel each other and the $\pi\Sigma$ component can contribute to the $\Lambda\gamma$ decay only through the slight isospin breaking. This means that the decay $\Lambda(1405)\to\Lambda\gamma$ is suitable for the study of the $\bar{K}N$ component in $\Lambda(1405)$. Fixing the $\Lambda(1405)$-$\pi\Sigma$ coupling constant from the usual decay of $\Lambda(1405)\to\pi\Sigma$, we show a relation between the absolute value of the $\bar{K}N$ compositeness for $\Lambda(1405)$ and the radiative decay width of $\Lambda(1405)\to\Lambda\gamma$ and $\Sigma^0\gamma$, and we find that large decay width to $\Lambda\gamma$ implies large $\bar{K}N$ compositeness for $\Lambda(1405)$. By using the "experimental" data on the radiative decay widths, which is based on an isobar model fitting of the K^-p atom data, we estimate the $\bar{K}N$ compositeness for $\Lambda(1405)$. We also discuss the pole position dependence of our relation on the $\Lambda(1405)$ radiative decay width and the effects of the two-pole structure for $\Lambda(1405)$.

DOI: 10.1103/PhysRevC.89.025202 PACS number(s): 13.40.Hq, 14.20.Jn, 21.45.−v

I. INTRODUCTION

Determination of the internal structure of hadrons is one of the most important issues in the physics of strong interaction. Especially exotic hadrons, which have different configurations from $q\bar{q}$ for mesons or qqq for baryons, are of interest because there is no clear experimental evidence of the existence of exotic hadrons while the fundamental theory of strong interaction, quantum chromodynamics (QCD), does not forbid such exotic hadrons [1]. Among others, $\Lambda(1405)$ is a "classical" example of the exotic hadron candidates. One of the remarkable properties for $\Lambda(1405)$ is its anomalously light mass. Actually in the $1/2^-$ state the lowest Λ excited state, $\Lambda(1405)$, is lighter than that of the nucleon excitation, $N(1535)$, although $\Lambda(1405)$ has a strange quark, which is heavier than up and down quarks.

As an interpretation of the $\Lambda(1405)$ properties, it has been considered that $\Lambda(1405)$ should be a $\bar{K}N$ quasi-bound state rather than a uds three-quark state [2,3]. This is reasonable, because $\Lambda(1405)$ exists just below the $\bar{K}N$ threshold and the interaction between $\bar{K}N$ is strongly attractive in the isospin $I=0$ channel. The idea that $\Lambda(1405)$ should be a $\bar{K}N$ quasibound state is recently reconfirmed by the so-called chiral unitary approach [4–8], which is based on the coupled-channels scattering unitarity with the interaction between hadrons restricted by the spontaneous chiral symmetry breaking in QCD, i.e., chiral perturbation theory. The chiral unitary approach reproduces the low-energy $\bar{K}N$ dynamics fairly well and dynamically generates $\Lambda(1405)$ without introducing explicit poles. In the experimental side, precise measurements have been recently performed so as to reveal the structure of $\Lambda(1405)$. For example, in Refs. [9,10] the $\Lambda(1405)$ line shape has been measured in the photoproduction, which is closely related to the underlying dynamics and the internal structure of $\Lambda(1405)$ [11]. In addition, there are discussions that the internal structure of $\Lambda(1405)$ can be extracted from, e.g., the coalescence of $\Lambda(1405)$ in heavy-ion collisions [12,13] and the exclusive production with high momentum π^- beam [14].

For the determination of the internal structures of exotic hadron candidates, one needs to pin down quantities which can be evidence of the exotic structure. The hadron yields in heavy-ion collisions [12,13] and the constituent-counting rule in high-energy exclusive production [14] are the examples. In addition to them, compositeness has been recently discussed as a quantity to determine the amount of two-body components in hadron resonances [15–19]. Here the compositeness is defined as a fraction of the two-body components in a resonance as well as a bound state and can be evaluated from the squared coupling constant of the resonance to the two-body states and a kinematical factor. Originally, whether a particle is elementary or composite was intensively discussed in the 1960s in terms of the field renormalization constant Z [20–22], which measures the bare state contribution rather than the composite state. A striking result is that a deuteron is indeed a proton-neutron bound state as shown in Ref. [23], in which a relation between the field renormalization constant of a deuteron and the scattering length and effective range in the proton-neutron scattering is established in the small binding energy limit in a model-independent way. Then attempts to investigate the structures of hadrons from the field renormalization constant Z were made in, e.g., Refs. [24–26]. Recently the

*sekihara@post.kek.jp

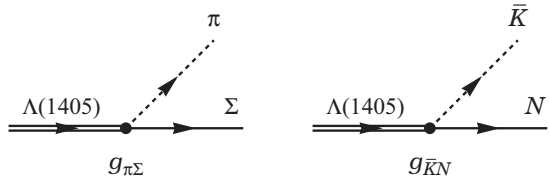

FIG. 1. Couplings of $\Lambda(1405)$ to the $\pi\Sigma$ (left) and $\bar{K}N$ (right) states. The $\Lambda(1405)$-$\pi\Sigma$ coupling constant $g_{\pi\Sigma}$ can be extracted from the decay width of $\Lambda(1405) \to \pi\Sigma$, but one cannot extract the $\Lambda(1405)$-$\bar{K}N$ coupling constant $g_{\bar{K}N}$ in a similar manner because $\Lambda(1405)$ exists below the $\bar{K}N$ threshold.

concept of the compositeness has been discussed in the context of the chiral unitary approach to determine internal structures of dynamically generated states [15]. Although the compositeness could be a complex value for resonances, it would be evidence of dominance of a two-body composite state or an elementary state, such as a non-$\pi\pi$ state for the ρ meson [16] or a non-$K\pi$ state for the K^* meson [17].

From these observations, we would like to determine the $\bar{K}N$ compositeness of $\Lambda(1405)$ from experimental information. Since the compositeness of $\Lambda(1405)$ can be evaluated from the coupling constant of $\Lambda(1405)$ (see Fig. 1) and a kinematic factor, i.e., derivation of the meson-baryon loop integral on the $\Lambda(1405)$ pole position, in order to determine the $\bar{K}N$ compositeness for $\Lambda(1405)$ we need to know the coupling constant of $\Lambda(1405)$ to $\bar{K}N$ as well as its pole position. However, while we can easily extract the $\Lambda(1405)$-$\pi\Sigma$ coupling constant from the $\Lambda(1405) \to \pi\Sigma$ decay, the $\Lambda(1405)$-$\bar{K}N$ coupling constant cannot be determined directly in experiments because $\Lambda(1405)$ exists below the $\bar{K}N$ threshold. Therefore, in order to determine the $\bar{K}N$ compositeness for $\Lambda(1405)$ we have to consider reactions which are sensitive to the $\Lambda(1405)$-$\bar{K}N$ coupling constant.

For such a reaction, we here treat the radiative decay of $\Lambda(1405)$: $\Lambda(1405) \to \Lambda\gamma$ and $\Sigma^0\gamma$ [27]. Since the $\Lambda(1405)$ radiative decay is closely related to the structure of $\Lambda(1405)$ as an $E1$ transition, up to now the radiative decay widths of $\Lambda(1405)$ have been evaluated in several models [28–38]. However, the decay widths have not been interpreted from the viewpoint of the $\bar{K}N$ composite contribution in detail. Therefore, in this study we give a relation between the $\bar{K}N$ compositeness for $\Lambda(1405)$ and the $\Lambda(1405)$ radiative decay width. Actually, as studied in Ref. [36], the $\Lambda(1405)$ radiative decay takes place mainly through the $\bar{K}N$ loop accompanied with the $\Lambda(1405)$-$\bar{K}N$ coupling. We will see that this fact is important to establish a relation between the $\bar{K}N$ compositeness for $\Lambda(1405)$ and the radiative decay width of $\Lambda(1405) \to \Lambda\gamma$.

This paper is organized as follows. In Sec. II we develop our formulation of the compositeness in the context of the chiral unitary approach. Then the radiative decay of the $\Lambda(1405)$ resonance is formulated in Sec. III. In Sec. IV we investigate possibilities to observe compositeness both for a $\bar{K}N$ bound state without strong decay and for the $\Lambda(1405)$ resonance. Section V is devoted to the conclusion of our study.

II. CHIRAL UNITARY APPROACH AND COMPOSITENESS

Recently the concept of compositeness has been intensively discussed in the context of the so-called chiral unitary approach [4–8] for dynamically generated states [15–19]. Therefore, we first review the formulation of the chiral unitary approach and the relation to the compositeness.

In the chiral unitary approach we construct an s-wave meson-baryon scattering amplitude $T_{ij}(s)$ by using the scattering unitarity, which is expressed as

$$\mathrm{Im}T_{ij}{}^{-1}(s) = \delta_{ij}\frac{\rho_i(s)}{2}\theta\left(s - s_i^{\mathrm{th}}\right), \tag{1}$$

where i and j denote channels, s is the Mandelstam variable, $\theta(x)$ is the Heaviside step function, and $s_i^{\mathrm{th}} = (m_i + M_i)^2$ is the threshold in the i channel with m_i and M_i being meson and baryon masses in channel i, respectively. The i-channel meson-baryon phase space $\rho_i(s)$ is defined as

$$\rho_i(s) \equiv \frac{M_i\lambda^{1/2}\left(s, m_i^2, M_i^2\right)}{4\pi s}, \tag{2}$$

with the Källen function $\lambda(x, y, z) = x^2 + y^2 + z^2 - 2xy - 2yz - 2zx$. Then, with neglect of the left-hand cut, one can construct a scattering equation in the Bethe-Salpeter type from the expression of the scattering unitarity (1) by using the N/D method [6]:

$$T_{ij}(s) = V_{ij}(s) + \sum_k V_{ik}(s)G_k(s)T_{kj}(s), \tag{3}$$

with an interaction kernel V_{ij} which coincides with the interactions taken from the chiral perturbation theory in the order matching scheme, and the dispersion integral G_i:

$$G_i(s) = -\tilde{a}_i(s_0) - (s - s_0)\int_{s_i^{\mathrm{th}}}^{\infty}\frac{ds'}{2\pi}\frac{\rho_i(s')}{(s' - s - i\epsilon)(s' - s_0)}. \tag{4}$$

Here $\tilde{a}_i$ is a subtraction constant at certain energy s_0, ϵ is an infinitesimal positive value, and $G_i(s)$ is known to equal, except for an infinite constant, the two-body loop integral. At the leading order of the chiral interaction for V_{ij}, which corresponds to the Weinberg-Tomozawa interaction plus s- and u-channel Born terms, only the subtraction constant in each channel is the model parameter. On the other hand, if one takes into account the next-to-leading order for V_{ij}, the low-energy constants in the interaction kernel also become model parameters.

By fitting the branching ratios of K^-p at its threshold, the chiral unitary approach can fairly well reproduce the existing experimental cross sections of the low-energy K^-p to various meson-baryon channels even only with the Weinberg-Tomozawa interaction [4–6]. Furthermore, the chiral unitary approach dynamically generates the $\Lambda(1405)$ resonance without introducing explicit resonance poles [8] and reproduces the $\Lambda(1405)$ spectrum in experiments. This approach supports the meson-baryon bound state picture for the $\Lambda(1405)$ resonance by revealing, e.g., a predominance of the meson-baryon component [39], its large-N_c scaling behavior [40,41], and its spatial size [42–44]. Recent studies within the chiral unitary approach as well as

experimental conditions on $\Lambda(1405)$ are summarized in the review article [45].

In addition, it is a prediction of the chiral unitary approach that $\Lambda(1405)$ is a superposition of two resonance poles in the energy region between $\pi\Sigma$ and $\bar{K}N$ thresholds [8]. One pole sitting in higher energy around 1420 MeV shows dominant coupling to $\bar{K}N$ and is expected to originate from the $\bar{K}N$ bound state while the other lower pole with large imaginary part strongly couples to $\pi\Sigma$ [46]. The higher pole around 1420 MeV is of interest because it means that one will observe $\Lambda(1405)$ spectrum which has a peak at 1420 MeV instead of the nominal 1405 MeV in the $\bar{K}N \to \pi\Sigma$ amplitude [8]. Indeed, an experiment of the $K^- d \to \pi\Sigma n$ reaction [47] gives support of the $\Lambda(1405)$ peak at 1420 MeV rather than 1405 MeV, which has been confirmed also by the theoretical calculations in the chiral unitary approach [48–51]. Also we note that a very recent experiment of the $\Lambda(1405)$ electroproduction [52] gives the $\Lambda(1405)$ line shape corresponding approximately to the predictions of a two-pole picture for $\Lambda(1405)$.

In general, the resonances as well as the bound states appear as poles of the scattering amplitude in the complex s plane. Actually poles of the dynamically generated states in the chiral unitary approach are expressed as

$$T_{ij}(s) = \frac{g_i g_j}{\sqrt{s} - Z_{\rm pole}} + T_{ij}^{\rm BG}. \tag{5}$$

where g_i is the coupling constant of the dynamically generated state to the channel i, $Z_{\rm pole} = M_{\rm R} - i\Gamma_{\rm R}/2$ is the pole position with $M_{\rm R}$ and $\Gamma_{\rm R}$ being interpreted as the mass and width of the state, respectively, and $T_{ij}^{\rm BG}$ is a background term which is regular at $\sqrt{s} \to Z_{\rm pole}$. Here we have defined the coupling constant g_i as the residue of the resonance pole with respect to $\sqrt{s}$ rather than s so that the $\Lambda(1405)$ field has dimension of mass to the power 3/2 in our notation. Now, according to the discussions on the scattering equations and field renormalizations, it was implied in Ref. [15] that the compositeness of the dynamically generated resonances with respect to the i channel, X_i, is related to the coupling constant g_i as

$$X_i = -g_i^2 \frac{dG_i}{d\sqrt{s}}(\sqrt{s} = Z_{\rm pole}). \tag{6}$$

The compositeness X_i approaches unity if the system is dominated by the i-channel two-body component, while it becomes zero if the system does not contain the i-channel two-body component. On the other hand, we can define the elementarity Z, which corresponds to the field renormalization constant and measures the fraction of the bare state contribution rather than the two-body state, as the residual part of the decomposition of unity:

$$Z = 1 - \sum_i X_i. \tag{7}$$

Then using the generalized Ward identity for the dynamically generated states proved in Ref. [43],

$$-\sum_{i,j}\left[g_i^2 \frac{dG_i}{d\sqrt{s}}\delta_{ij} + g_i G_i \frac{dV_{ij}}{d\sqrt{s}} G_j g_j\right]_{\sqrt{s}=Z_{\rm pole}} = 1, \tag{8}$$

we can express the elementarity as

$$Z = -\sum_{i,j} g_i G_i \frac{dV_{ij}}{d\sqrt{s}} G_j g_j \Big|_{\sqrt{s}=Z_{\rm pole}}. \tag{9}$$

An important point to be noted is that the compositeness X_i is expressed as the squared coupling constant g_i^2, which contains information on the dynamics, times the derivative of the dispersion integral G_i, which depends only on the kinematics. We also note that each X_i as well as the elementarity Z, which take real values for bound states without decay width, become complex for resonance states. However, the sum of the compositeness and the elementarity is exactly unity as in Eq. (7). In this sense we can extract the amount of the i channel component for the resonance states from the compositeness X_i.

To conclude this section we demonstrate the $\pi\Sigma$ compositeness of $\Lambda(1405)$ from the usual decay of $\Lambda(1405)$, $\Lambda(1405) \to \pi\Sigma$, assuming the isospin symmetry both for the coupling constant and the hadron masses. The decay width $\Gamma_{\Lambda(1405)}$ is related to the $\pi\Sigma$ coupling in the particle basis, $g_{\pi\Sigma} = g_{\pi^+\Sigma^-} = g_{\pi^-\Sigma^+} = g_{\pi^0\Sigma^0}$, in the following form:

$$\Gamma_{\Lambda(1405)} = 3 \times \frac{p_{\rm cm} M_\Sigma}{2\pi M_{\Lambda(1405)}} |g_{\pi\Sigma}|^2, \tag{10}$$

where $p_{\rm cm}$ is the center-of-mass three-momentum of the final-state π, M_Σ is the averaged Σ baryon mass, and the factor 3 corresponds to the three possible final states: $\pi^+\Sigma^-$, $\pi^-\Sigma^+$, and $\pi^0\Sigma^0$. From the experimental data $M_{\Lambda(1405)} = 1405$ MeV and $\Gamma_{\Lambda(1405)} = 50$ MeV of the Particle Data Group [1], we have $|g_{\pi\Sigma}| = 0.91$. Then, the absolute value of the $\pi\Sigma$ compositeness can be evaluated as

$$|X_{\pi\Sigma}| = 3 \times \left| g_{\pi\Sigma}^2 \frac{dG_{\pi\Sigma}}{d\sqrt{s}}(\sqrt{s} = Z_{\rm pole}) \right| = 0.19, \tag{11}$$

where $Z_{\rm pole} = M_{\Lambda(1405)} - i\Gamma_{\Lambda(1405)}/2$.[1] This means that the $\pi\Sigma$ component in the $\Lambda(1405)$ resonance is not dominant and hence the $\Lambda(1405)$ should originate some dynamics rather than the $\pi\Sigma$ interaction. In a similar manner we could evaluate the $\bar{K}N$ compositeness of $\Lambda(1405)$, but it is impossible because $\Lambda(1405)$ exists below the $\bar{K}N$ threshold and the decay to $\bar{K}N$ is invisible. Furthermore, there are no direct relations between the $\bar{K}N$ compositeness and observables such as the $K^- p$ scattering length in contrast to the deuteron case. Therefore, in order to obtain information on the $\bar{K}N$ component inside $\Lambda(1405)$, we have to observe other decay modes which are sensitive to the $\Lambda(1405)$-$\bar{K}N$ coupling constant, such as the radiative decay.

[1] We note that the pole position of $\Lambda(1405)$, which is necessary to evaluate the compositeness (6), is not well determined from experiments. Actually the interference between $\Lambda(1405)$ and the $I = 1$ background could shift the $\Lambda(1405)$ peak position in the spectrum as in Refs. [9–11] and moreover the chiral unitary approach predicts the two-pole structure for $\Lambda(1405)$ [8]. Here we simply assume that the pole position is obtained from the mass and width in the Particle Data Group. In this study we will discuss the pole position dependence of the $\Lambda(1405)$ radiative decay width and the effects of the two-pole structure for $\Lambda(1405)$.

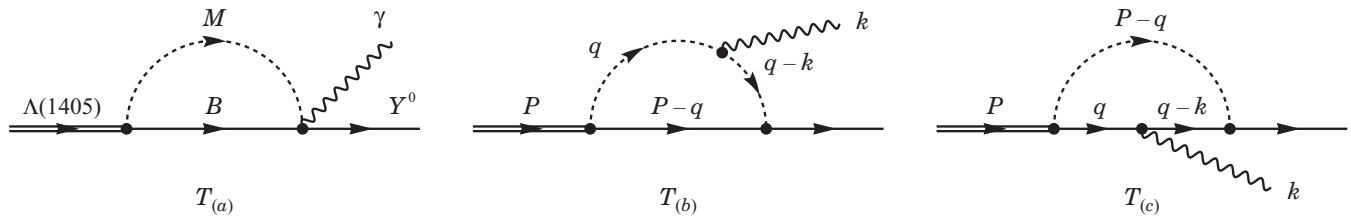

FIG. 2. Feynman diagrams for the $\Lambda(1405)$ radiative decay. Here M and B in the left diagram denote mesons and baryons, respectively, and P, q, $P-q$, k, and $q-k$ in the middle and right diagrams indicate the momenta carried by the corresponding mesons, baryons, and photons.

III. FORMULATION OF RADIATIVE DECAY

Now let us formulate the radiative decay of $\Lambda(1405)$: $\Lambda(1405) \to Y^0\gamma$ with $Y^0 = \Lambda, \Sigma^0$. Our formulation is based on that developed in Ref. [36]. Here the radiative decay widths are perturbatively calculated and hence we use the same coupling constants in the formulation as those obtained in the strong interaction without the electromagnetic interaction; i.e., those in Eq. (5). The relevant diagrams for the radiative decay are shown in Fig. 2, and from the Feynman rules summarized in Appendix A each diagram gives the decay amplitude as

$$-iT_{(a)} = -e\sigma_\mu \epsilon_\nu^* \sum_i g_i Q_{M_i} \tilde{V}_{iY^0} g^{\mu\nu} G_i(P), \tag{12}$$

$$-iT_{(b)} = +e\sigma_\mu \epsilon_\nu^* \sum_i g_i Q_{M_i} \tilde{V}_{iY^0} D^{\mu\nu}_{iY^0(1)}(P,k), \tag{13}$$

$$-iT_{(c)} = +e\sigma_\mu \epsilon_\nu^* \sum_i g_i Q_{B_i} \tilde{V}_{iY^0} D^{\mu\nu}_{iY^0(2)}(P,k), \tag{14}$$

where e is the elementary charge, σ^μ is defined as $\sigma^\mu = (0, \boldsymbol{\sigma})$ with the Pauli matrices σ^i $(i = 1, 2, 3)$ for baryon spinors, and $\epsilon^{*\mu}$ is the polarization of the final-state photon. Inside the summations with respect to the channel i, g_i is the coupling constant of $\Lambda(1405)$ to the channel i, Q_{M_i} and Q_{B_i} are charges of the meson and baryon in channel i, respectively, and $\tilde{V}_{iY^0}$ is the meson-baryon-baryon (MBB) coupling strength:

$$\tilde{V}_{iY^0} = \alpha_{iY^0} \frac{D+F}{2f} + \beta_{iY^0} \frac{D-F}{2f}, \tag{15}$$

with SU(3) coefficients α and β, parameters D and F, and the meson decay constant f. The loop integrals G_i, $D^{\mu\nu}_{iY^0(1)}$, and $D^{\mu\nu}_{iY^0(2)}$ are defined as

$$G_i(P) \equiv i \int \frac{d^4q}{(2\pi)^4} \frac{1}{q^2 - m_i^2} \frac{2M_i}{(P-q)^2 - M_i^2}, \tag{16}$$

$$D^{\mu\nu}_{iY^0(1)}(P,k) \equiv i \int \frac{d^4q}{(2\pi)^4} \frac{(q-k)^\mu (2q-k)^\nu}{\left[(q-k)^2 - m_i^2\right]\left(q^2 - m_i^2\right)} \frac{2M_i}{(P-q)^2 - M_i^2}, \tag{17}$$

$$D^{\mu\nu}_{iY^0(2)}(P,k) \equiv i \int \frac{d^4q}{(2\pi)^4} \frac{2M_i (P-q)^\mu (2q-k)^\nu}{\left[(q-k)^2 - M_i^2\right]\left(q^2 - M_i^2\right)} \frac{1}{(P-q)^2 - m_i^2}, \tag{18}$$

with P^μ and k^μ being the momenta of the initial-state $\Lambda(1405)$ and final-state photon, respectively. Here the squared masses in the denominators are implicitly assumed to be added by $-i\epsilon$, where ϵ is an infinitesimal positive value: $m^2 \to m^2 - i\epsilon$ and $M^2 \to M^2 - i\epsilon$. In this study the relevant channels with nonzero charge are $K^- p$, $\pi^+\Sigma^-$, $\pi^-\Sigma^+$, and $K^+\Xi^-$, and the values of α_{iY^0} and β_{iY^0} relevant to this study are listed in Table I. Since we have a relation $Q_{B_i} = -Q_{M_i}$ for the meson-baryon states coupled to the zero-charge $\Lambda(1405)$, the decay amplitudes are collected to give the total decay amplitude,

$$T_{\Lambda(1405)\to Y^0\gamma} = -ie\sigma_\mu \epsilon_\nu^* \sum_i g_i Q_{M_i} \tilde{V}_{iY^0} H^{\mu\nu}_{iY^0}(P,k), \tag{19}$$

with the summation of the loop integrals,

$$H^{\mu\nu}_{iY^0}(P,k) \equiv g^{\mu\nu} G_i(P) - D^{\mu\nu}_{iY^0(1)}(P,k) + D^{\mu\nu}_{iY^0(2)}(P,k). \tag{20}$$

For the evaluation of the loop integrals $H_i^{\mu\nu}$, we take the strategy developed in Refs. [36,53–57] based on the symmetries. Namely, since we have only P^μ and k^μ to describe the Lorentz indices μ and ν with respect to $H_i^{\mu\nu}$, the general form of $H_i^{\mu\nu}$ should be expressed as

$$H^{\mu\nu}_{iY^0} = a_{iY^0} g^{\mu\nu} + b_{iY^0} P^\mu P^\nu + c_{iY^0} P^\mu k^\nu + d_{iY^0} k^\mu P^\nu + e_{iY^0} k^\mu k^\nu. \tag{21}$$

Then, since we consider an on-shell photon in the final state, we have the transverse polarization, $\epsilon_\nu^* k^\nu = 0$. This means that the terms proportional to c_{iY^0} and e_{iY^0} vanish and do not contribute to the radiative decay, hence we do not consider them in the following. Furthermore, since the Ward identity constrains $k_\nu H^{\mu\nu}_{iY^0} = 0$ in each channel i (see Appendix B), we have

$$a_{iY^0} k^\mu + b_{iY^0} P^\mu (P\cdot k) + d_{iY^0} k^\mu (P\cdot k) = 0. \tag{22}$$

TABLE I. SU(3) coupling strengths for the MBB vertex.

i	$K^- p$	$\pi^+\Sigma^-$	$\pi^-\Sigma^+$	$K^+\Xi^-$
$\alpha_{i\Lambda}$	$-2/\sqrt{3}$	$1/\sqrt{3}$	$1/\sqrt{3}$	$1/\sqrt{3}$
$\beta_{i\Lambda}$	$1/\sqrt{3}$	$1/\sqrt{3}$	$1/\sqrt{3}$	$-2/\sqrt{3}$
$\alpha_{i\Sigma^0}$	0	1	-1	1
$\beta_{i\Sigma^0}$	1	-1	1	0

Here we can take values of P^μ and k^μ independently, so the equation implies $b_{iY^0} = 0$ and

$$a_{iY^0} + d_{iY^0}(P \cdot k) = 0. \tag{23}$$

This relation has a special meaning. Suppose that we would like to calculate the term a_{iY^0}. Then Eq. (23) tells us that evaluating a_{iY^0} is equivalent to evaluating d_{iY^0}. Furthermore, although each loop integral contributing to a_{iY^0} such as $G_i(P)$ diverges, Eq. (23) indicates that all divergences cancel each other to be a finite value, because d_{iY^0} is obviously finite as one can see from the dimension counting. At last we consider $\Lambda(1405)$ at rest, $P^\mu = (M_{\Lambda(1405)}, \mathbf{0})$, and the Coulomb gauge $\epsilon^0 = 0$, so the term d_{iY^0} does not contribute to the total amplitude due to $\epsilon^*_\nu P^\nu = 0$ and hence we only need a_{iY^0}.

From the above discussion, what we have to calculate is the term proportional to $k^\mu P^\nu$ in $g^{\mu\nu}G_i(P)$, $D^{\mu\nu}_{iY^0(1)}$, and $D^{\mu\nu}_{iY^0(2)}$ to translate d_{iY^0} into a_{iY^0} via Eq. (23). Since the first one does not have a factor of $k^\mu P^\nu$ but $g^{\mu\nu}$, we may not evaluate the first one. Thus we concentrate on the second and third ones. Using the Feynman parametrization

$$\frac{1}{ABC} = \int_0^1 dx \int_0^1 dy \frac{2x}{[Axy + Bx(1-y) + C(1-x)]^3}, \tag{24}$$

and the four-dimensional integration

$$\int \frac{d^4q}{(2\pi)^4} \frac{i}{(q^2 - S)^3} = \frac{1}{32\pi^2 S}, \tag{25}$$

we evaluate the term proportional to $k^\mu P^\nu$ in $D^{\mu\nu}_{iY^0(1)}$ as

$$D^{\mu\nu}_{iY^0(1)}|_{k^\mu P^\nu} = -\frac{M_i k^\mu P^\nu}{4\pi^2} \int_0^1 dx \int_0^1 dy \frac{x(1-x)(1-xy)}{S(x,y)}, \tag{26}$$

where $S(x, y)$ is defined as

$$S(x,y) \equiv xm^2 + (1-x)M^2 - x(1-x)P^2 + 2x(1-x)yP \cdot k. \tag{27}$$

In a similar manner, the term proportional to $k^\mu P^\nu$ in $D^{\mu\nu}_{iY^0(2)}$ is evaluated as

$$D^{\mu\nu}_{iY^0(2)}\big|_{k^\mu P^\nu} = -\frac{M_i k^\mu P^\nu}{4\pi^2} \int_0^1 dx \int_0^1 dy \frac{x(1-x)^2 y}{S(x,y)}. \tag{28}$$

As a result, we have

$$d_{iY^0}(\sqrt{s}) = \frac{M_i}{4\pi^2} \int_0^1 dx \int_0^1 dy \frac{x(1-x)(1-y)}{S(x,y)} = \frac{M_i}{4\pi^2} \frac{1}{2P \cdot k} \int_0^1 dx \left[-1 + (1-y_0) \ln\left(\frac{1-y_0}{-y_0}\right)\right], \tag{29}$$

where $\sqrt{s}$ is the total energy, $P^\mu = (\sqrt{s}, \mathbf{0})$, to be fixed as the $\Lambda(1405)$ mass $\sqrt{s} = M_{\Lambda(1405)}$ and the y integration is performed in the last line of the equation and y_0 is defined as

$$y_0(\sqrt{s}) \equiv -\frac{xm^2 + (1-x)M^2 - x(1-x)s}{2x(1-x)P \cdot k}. \tag{30}$$

We note that the logarithmic term in Eq. (29) generates an imaginary part for $0 < y_0 < 1$. Then, by using Eq. (23) a_{iY^0} is evaluated as

$$a_{iY^0}(\sqrt{s}) = -\frac{M_i}{8\pi^2} \int_0^1 dx \left[-1 + (1-y_0) \ln\left(\frac{1-y_0}{-y_0}\right)\right]. \tag{31}$$

As a consequence, the total decay amplitude at the $\Lambda(1405)$ rest frame in the Coulomb gauge becomes

$$T_{\Lambda(1405)\to Y^0\gamma} = i\boldsymbol{\sigma} \cdot \boldsymbol{\epsilon}^* W_{Y^0\gamma}(\sqrt{s}), \tag{32}$$

with

$$W_{Y^0\gamma}(\sqrt{s}) \equiv e \sum_i g_i Q_{M_i} \tilde{V}_{iY^0} a_{iY^0}(\sqrt{s}). \tag{33}$$

Finally the radiative decay width is expressed as

$$\Gamma_{Y^0\gamma} = \frac{p'_{\rm cm} M_{Y^0}}{\pi M_{\Lambda(1405)}} \left| W_{Y^0\gamma}(\sqrt{s} = M_{\Lambda(1405)}) \right|^2, \tag{34}$$

where $p'_{\rm cm}$ is the center-of-mass three-momentum of the final-state photon. We note again that each loop integral, $G(P)$, $D^{\mu\nu}_{i(1)}$, or $D^{\mu\nu}_{i(2)}$, diverges, but the sum of them gives a finite value as seen in Eq. (31). Throughout this study we take $D + F = 1.26$, $D - F = 0.33$, and $f = 1.15 f_\pi$ with the pion decay constant $f_\pi = 93$ MeV.

IV. RESULTS

In this section we calculate the radiative decay width of $\Lambda(1405)$ as a function of the $\bar{K}N$ compositeness $X_{\bar{K}N}$. Here we use the physical hadron masses, which breaks slightly the isospin symmetry, but assume the isospin symmetry for the coupling constants of $\Lambda(1405)$ to each channel except for the coupling constants evaluated in the chiral unitary approach. In order to understand the behavior of the decay width, we first consider a $\bar{K}N$ bound state in the $I = 0$ channel without couplings to other channels in Sec. IV A, and then the radiative decay width of $\Lambda(1405)$ is evaluated in Sec. IV B. We also discuss the pole position dependence of the $\Lambda(1405)$ radiative decay width and the effects of the two-pole structure for $\Lambda(1405)$ in Sec. IV C.

A. Radiative decay of a bound state

We firstly consider a $\bar{K}N(I = 0)$ bound state by taking into account only the K^-p and $\bar{K}^0n$ channels while switching off the couplings to other channels such as $\pi\Sigma$. Hence, the state is described only by K^-p and $\bar{K}^0n$, and the radiative decay takes place only through the K^-p loop. Here we assume isospin symmetry for the coupling constant: $g_{\bar{K}N} = g_{K^-p} = g_{\bar{K}^0n}$. We take $M_{\rm B}$ as the mass of the $\bar{K}N$ bound state, which is real and positive, and measure the binding energy $B_{\rm E}$ from the mean value of the K^-p and $\bar{K}^0n$ thresholds:

$$B_{\rm E} = \frac{M_{K^-} + M_p + M_{\bar{K}^0} + M_n}{2} - M_{\rm B}. \tag{35}$$

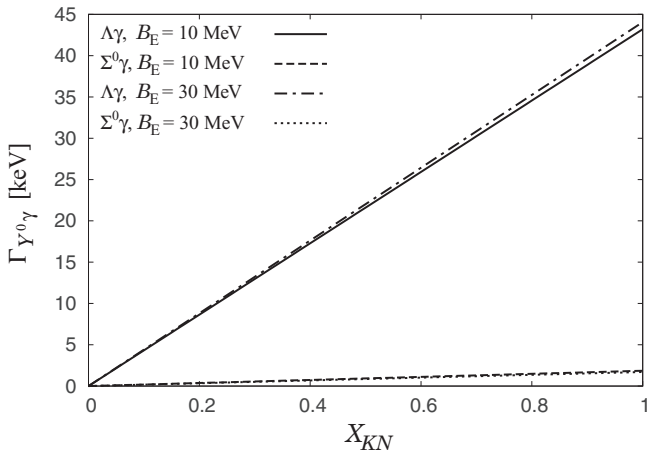

FIG. 3. Radiative decay width of a $\bar{K}N$ bound state as a function of the $\bar{K}N$ compositeness.

In this condition the $\bar{K}N$ compositeness for the bound state, which takes a real value, can be evaluated as

$$X_{\bar{K}N} = -g_{\bar{K}N}^2 \left[\frac{dG_{K^-p}}{d\sqrt{s}} + \frac{dG_{\bar{K}^0n}}{d\sqrt{s}} \right]_{\sqrt{s}=M_B}. \tag{36}$$

This indicates that for a given binding energy the coupling constant $g_{\bar{K}N}$ and the compositeness $X_{\bar{K}N}$ have one-to-one correspondence. In addition, since the model parameter of the radiative decay width is only the coupling constant $g_{\bar{K}N}$, we have one-to-one correspondence between the $\bar{K}N$ compositeness and the radiative decay width as well as the $\bar{K}N$ coupling constant and the radiative decay width. Therefore, one can evaluate the radiative decay width as a function of the $\bar{K}N$ compositeness $X_{\bar{K}N}$ through the relation (36). Since the mass of $\Lambda(1405)$ is 1405 MeV from the Particle Data Group [1] while the chiral unitary approach suggests a real part of the $\Lambda(1405)$ pole position around 1420 MeV [8], we choose two binding energies $B_E = 10$ MeV ($M_B = 1425$ MeV) and $B_E = 30$ MeV ($M_B = 1405$ MeV).

In Fig. 3 we show the radiative decay width of the $\bar{K}N(I = 0)$ bound state as a function of the $\bar{K}N$ compositeness with two binding energies $B_E = 10$ and 30 MeV. As on can see, the radiative decay width both to $\Lambda\gamma$ and $\Sigma^0\gamma$ is proportional to the $\bar{K}N$ compositeness $X_{\bar{K}N}$ since both the decay width and the compositeness are proportional to the squared coupling constant $g_{\bar{K}N}^2$. Furthermore, it is interesting that the decay to $\Lambda\gamma$ is dominant while the decay to $\Sigma^0\gamma$ is quite small. This behavior can be understood by the coupling strengths of $K^-p\Lambda$ and $K^-p\Sigma^0$. Namely, the flavor SU(3) symmetry gives the coupling strengths

$$\tilde{V}_{K^-p\Lambda} = -\frac{D+3F}{2\sqrt{3}f} \approx -\frac{0.63}{f}, \tag{37}$$

$$\tilde{V}_{K^-p\Sigma^0} = \frac{D-F}{2f} \approx \frac{0.17}{f}, \tag{38}$$

This difference gives a very large ratio $\sim$14 for the radiative decay width $\Gamma_{\Lambda\gamma}/\Gamma_{\Sigma^0\gamma}$. Figure 3 means that we have established a relation between the $\bar{K}N$ compositeness inside the $\bar{K}N(I = 0)$ bound state and the radiative decay width.

On the other hand, the binding energy dependence of the radiative decay width is very small and almost invisible. This indicates that the behavior of the squared loop integral $a_{K^-pY^0}^2$ with respect to the energy $\sqrt{s}$ is very similar to that of $-dG_{K^-p}/d\sqrt{s}$ and $-dG_{\bar{K}^0n}/d\sqrt{s}$ in the energy region $1400 < \sqrt{s} < 1430$ MeV, and hence for a given $X_{\bar{K}N}$ [see Eq. (36)] at $\sqrt{s} = M_B$ the radiative decay width $\Gamma \propto g_{\bar{K}N}^2 a_{K^-pY^0}^2(\sqrt{s} = M_B)$ takes almost similar values independently of the bound state mass M_B. In other words, since both G and $dG/d\sqrt{s}(<0)$ monotonically decrease as functions of $\sqrt{s}$ below the threshold, for a fixed $X_{\bar{K}N}$ a larger binding energy leads to smaller $-dG/d\sqrt{s}$ and hence larger $g_{\bar{K}N}^2$. Then, since the energy dependence of $a_{K^-pY^0}^2$ is very similar to that of $-dG_{K^-p}/d\sqrt{s} - dG_{\bar{K}^0n}/d\sqrt{s}$, a larger binding energy leads to the smaller $a_{K^-pY^0}^2$, and hence for a fixed $X_{\bar{K}N}$ the binding energy dependence of $g_{\bar{K}N}^2 a_{K^-pY^0}^2$ is almost canceled. This fact will be more important when we consider the $\Lambda(1405)$ resonance. Namely, we expect that the radiative decay width of $\Lambda(1405)$ can be evaluated as a function of the $\bar{K}N$ compositeness almost independently of the $\Lambda(1405)$ pole position, which is not well determined experimentally at present.

B. Radiative decay of Λ(1405)

In the previous subsection we have studied the radiative decay of a $\bar{K}N(I = 0)$ bound state by taking into account only the K^-p and $\bar{K}^0n$ channels while switching off the couplings to other channels. As a result we have established a relation between the $\bar{K}N$ compositeness for the $\bar{K}N$ bound state and the radiative decay width. In this subsection we extend our discussion to the $\Lambda(1405)$ resonance in multiple channels and investigate whether or not we can establish a relation between the $\bar{K}N$ compositeness for $\Lambda(1405)$ and the $\Lambda(1405)$ radiative decay width.

Before evaluating the radiative decay width as a function of the $\bar{K}N$ compositeness for $\Lambda(1405)$, we first evaluate the $\Lambda(1405)$ radiative decay width in the chiral unitary approach with the recently updated parameters [58,59]. In Refs. [58,59] two poles corresponding to $\Lambda(1405)$ are reconfirmed, and the pole positions of $\Lambda(1405)$, the coupling constants to meson-baryon channels on the pole positions, and the resulting radiative decay widths, which correspond to the updated values with respect to the previous study [36], are listed in Table II. As one can see, the radiative decay width to $\Lambda\gamma$ is larger than that to $\Sigma^0\gamma$ for the higher $\Lambda(1405)$ pole whereas decay to $\Sigma^0\gamma$ is dominant for the lower pole. This behavior comes from the structure of the meson-baryon-baryon coupling $\tilde{V}$ as discussed in Ref. [36]. Namely, the $K^-p\Lambda$ coupling strength $\tilde{V}_{K^-p\Lambda}$ is large compared to the $K^-p\Sigma^0$ one $\tilde{V}_{K^-p\Sigma^0}$, as we have already shown in Eqs. (37) and (38) in the previous subsection. On the other hand, the $\pi^\pm\Sigma^\mp\Lambda$ couplings are found to be

$$\tilde{V}_{\pi^+\Sigma^-\Lambda} = \tilde{V}_{\pi^-\Sigma^+\Lambda} = \frac{D}{\sqrt{3}f} \approx \frac{0.46}{f}, \tag{39}$$

TABLE II. Radiative decay width of $\Lambda(1405)$ in the chiral unitary approach with the recently updated parameters [58,59].

	$\Lambda(1405)$, higher pole	$\Lambda(1405)$, lower pole
$Z_{\rm pole}$ (MeV)	$1424 - 26i$	$1381 - 81i$
g_{K^-p}	$2.25 + 0.87i$	$0.91 - 1.89i$
$g_{\pi^+\Sigma^-}$	$0.57 + 1.00i$	$1.37 - 1.28i$
$g_{\pi^-\Sigma^+}$	$0.62 + 1.06i$	$1.48 - 1.28i$
$g_{K^+\Xi^-}$	$0.23 + 0.08i$	$0.02 - 0.26i$
$\Gamma_{\Lambda\gamma}$ (keV)	96	31
$\Gamma_{\Sigma^0\gamma}$ (keV)	60	94

and hence, due to the opposite sign of the charge $Q_{\pi^+} = -Q_{\pi^-} = 1$, for the $\pi\Sigma$ component tiny isospin breakings in the loop integral $a_{\pi^\pm\Sigma^\mp}$ and in the coupling constant $g_{\pi\Sigma}$ can contribute to the decay to $\Lambda\gamma$. Therefore, the decay to $\Lambda\gamma$ is dominated by the $\bar{K}N$ component. Similarly, for the decay to $\Sigma^0\gamma$ we have

$$\tilde{V}_{\pi^+\Sigma^-\Sigma^0} = -\tilde{V}_{\pi^-\Sigma^+\Sigma^0} = \frac{F}{f} \approx \frac{0.47}{f}, \tag{40}$$

which are larger than the $K^-p\Sigma^0$ coupling strength (38), and the constructive interference between $\pi^\pm\Sigma^\mp$ does take place. As a result, the $\Sigma^0\gamma$ decay is dominated by the $\pi\Sigma$ component. Then, as listed in Table II, the higher pole dominantly couples to the $\bar{K}N$ channel while the lower pole strongly couples to the $\pi\Sigma$ channel. These coupling strengths lead to the large $\Gamma_{\Lambda\gamma}/\Gamma_{\Sigma^0\gamma}$ in the higher pole and to the small $\Gamma_{\Lambda\gamma}/\Gamma_{\Sigma^0\gamma}$ in the lower pole. We note that the interference between K^-p and $\pi^\pm\Sigma^\mp$ in $\Gamma_{\Lambda\gamma}$ is constructive both for the higher and lower $\Lambda(1405)$ poles, while the interference in $\Gamma_{\Sigma^0\gamma}$ is constructive (destructive) for the higher (lower) pole. In addition, we also note that for both poles the couplings to the $K\Xi$ channel are small and hence the $K\Xi$ component can only scarcely contribute to the radiative decay.

Bearing these discussions in mind, we calculate the radiative decay width of $\Lambda(1405)$ as a function of the $\bar{K}N$ compositeness for $\Lambda(1405)$. Here we first fix the $\Lambda(1405)$ pole position by using the mass and width taken from the Particle Data Group [1]: $Z_{\rm pole} = M_{\Lambda(1405)} - i\Gamma_{\Lambda(1405)}/2$ with $M_{\Lambda(1405)} = 1405$ MeV and $\Gamma_{\Lambda(1405)} = 50$ MeV. Then we will discuss later the pole position dependence of the relation between the radiative decay width and the $\bar{K}N$ compositeness. The $\bar{K}N$ compositeness $X_{\bar{K}N}$ is related to the $\bar{K}N$ coupling constant in the particle basis, $g_{\bar{K}N} = g_{K^-p} = g_{\bar{K}^0n}$, as

$$X_{\bar{K}N} = -g_{\bar{K}N}^2 \left[\frac{dG_{K^-p}}{d\sqrt{s}} + \frac{dG_{\bar{K}^0n}}{d\sqrt{s}}\right]_{\sqrt{s}=Z_{\rm pole}}. \tag{41}$$

However, since $\Lambda(1405)$ is a resonance state, the compositeness $X_{\bar{K}N}$ as well as the coupling constant $g_{\bar{K}N}$ are in general complex. Therefore, in this study, in order to evaluate the radiative decay width as a function of a real variable, we use Eq. (41) to relate the absolute value of the compositeness $|X_{\bar{K}N}|$ and that of the coupling constant $|g_{\bar{K}N}|$. We note that, although the absolute value of the compositeness $|X_{\bar{K}N}|$ as well as the complex compositeness for the $\Lambda(1405)$ resonance cannot be interpreted as a probability of finding the $\bar{K}N$ component, it will be helpful information and a guide to elucidating the structure of $\Lambda(1405)$. For instance, the large absolute value of the $\bar{K}N$ compositeness $|X_{\bar{K}N}|$ is a necessary condition for the $\bar{K}N$ bound state picture for $\Lambda(1405)$. In this strategy, for a given $|X_{\bar{K}N}|$ we can uniquely determine $|g_{\bar{K}N}|$. On the other hand, the $\pi\Sigma$ coupling constant can be fixed from the usual $\Lambda(1405) \to \pi\Sigma$ decay, and from Eq. (10) we take $|g_{\pi\Sigma}| = 0.91$. Finally, since the $K\Xi$ component inside $\Lambda(1405)$ should be small, we neglect the $K\Xi$ coupling: $g_{K^+\Xi^-} = g_{K^0\Xi^0} = 0$.

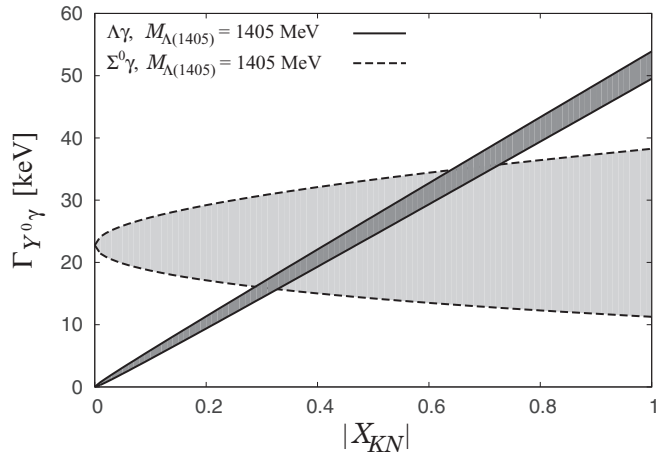

FIG. 4. Radiative decay width of $\Lambda(1405)$ as a function of the absolute value of the $\bar{K}N$ compositeness. The $\Lambda(1405)$ mass is fixed as $M_{\Lambda(1405)} = 1405$ MeV.

Although we have fixed the absolute values of the coupling constants $|g_{\bar{K}N}|$ and $|g_{\pi\Sigma}|$, the relative phase between $g_{\bar{K}N}$ and $g_{\pi\Sigma}$ is not known and hence one cannot calculate the interference term.[2] Therefore, in order to evaluate the radiative decay width, we use a procedure to calculate both the maximally constructive and maximally destructive terms. Namely, we calculate decay amplitudes of

$$W^\pm_{Y^0\gamma} = e\big(|g_{\bar{K}N}| \times \big|\tilde{V}_{K^-pY^0}a_{K^-pY^0}\big| \pm |g_{\pi\Sigma}| \times \big|\tilde{V}_{\pi^+\Sigma^-Y^0}a_{\pi^+\Sigma^-Y^0} - \tilde{V}_{\pi^-\Sigma^+Y^0}a_{\pi^-\Sigma^+Y^0}\big|\big) \tag{42}$$

and evaluate the decay width (34) so as to show the allowed range for the radiative decay width for each absolute value of the $\bar{K}N$ compositeness $|X_{\bar{K}N}|$.

The results of the allowed range of the $\Lambda(1405)$ radiative decay widths are shown in Fig. 4 as functions of the absolute value of the $\bar{K}N$ compositeness $|X_{\bar{K}N}|$. As one can see from the figure, the range of the radiative decay width to $\Lambda\gamma$ increases almost linearly with a small band as $|X_{\bar{K}N}|$ increases. This is because the $\pi^+\Sigma^-$ and $\pi^-\Sigma^+$ components largely cancel each other and only a tiny isospin breaking part can contribute to the $\Lambda\gamma$ decay. This fact indicates that the radiative decay $\Lambda(1405) \to \Lambda\gamma$ is suited to study the

[2]Since we assume the isospin symmetry for the coupling constants, $g_{\pi\Sigma} = g_{\pi^+\Sigma^-} = g_{\pi^-\Sigma^+} = g_{\pi^0\Sigma^0}$ and so on, the relative phase between $\pi^+\Sigma^-$ and $\pi^-\Sigma^+$ is already determined.

$\bar{K}N$ component inside $\Lambda(1405)$. Especially a large decay width $\Gamma_{\Lambda\gamma}$ directly indicates a large absolute value of the $\bar{K}N$ compositeness $|X_{\bar{K}N}|$, and hence implies a large $\bar{K}N$ component inside $\Lambda(1405)$. On the other hand, $\Sigma^0\gamma$ decay is dominated by the $\pi\Sigma$ component and hence the decay width becomes $\Gamma_{\Sigma^0\gamma} \sim 23$ keV even for $|X_{\bar{K}N}| = 0$. Then, as $|X_{\bar{K}N}|$ grows the values of $W^{\pm}$ are more separated from each other and the allowed range for the $\Sigma^0\gamma$ decay width is expanded. Here we note that the maximal and minimal values of $\Gamma_{\Sigma^0\gamma}$ become $\sim$40 and 10 keV, respectively, for $|X_{\bar{K}N}| = 1$, so we could conclude that $|X_{\bar{K}N}|$ should be large if the decay width for $\Sigma^0\gamma$ would be considerably large or considerably small.

By using the relation in Fig. 4 we can estimate the $\bar{K}N$ compositeness from the $\Lambda(1405)$ radiative decay width. Actually, there are "experimental" data on the $\Lambda(1405)$ radiative decay width evaluated from an isobar model fitting of the decays of the K^-p atom [27]: $\Gamma_{\Lambda\gamma} = 27 \pm 8$ keV and $\Gamma_{\Sigma^0\gamma} = 10 \pm 4$ or 23 ± 7 keV. From these "experimental" values we can estimate the $\bar{K}N$ compositeness by using the relation in Fig. 4. As a result, we extract $|X_{\bar{K}N}| = 0.5 \pm 0.2$ from $\Gamma_{\Lambda\gamma} = 27 \pm 8$ keV, $|X_{\bar{K}N}| > 0.5$ from $\Gamma_{\Sigma^0\gamma} = 10 \pm 4$ keV, while $|X_{\bar{K}N}|$ can have an arbitrary value within $\Gamma_{\Sigma^0\gamma} = 23 \pm 7$ keV. These results suggest that the absolute value of the $\bar{K}N$ compositeness is $|X_{\bar{K}N}| \gtrsim 0.5$, which implies that $\bar{K}N$ seems to be the largest component inside $\Lambda(1405)$.

Finally we make several comments. In this study we use the Particle Data Group value to determine the pole position of $\Lambda(1405)$ as $Z_{\rm pole} = M_{\Lambda(1405)} - i\Gamma_{\Lambda(1405)}/2$. However, the $\Lambda(1405)$ pole position is not well determined, although the compositeness (41) should be evaluated on the $\Lambda(1405)$ pole position. This may lead to an ambiguity of the relation between the $\bar{K}N$ compositeness and the radiative decay width shown in Fig. 4. This point is discussed in the next subsection together with the effects of the two-pole structure for $\Lambda(1405)$.

In addition, we have neglected the bare state contribution of $\Lambda(1405)$ to the radiative decay. Actually, even if the $\Lambda(1405)$ would be dominated by a quark bound state such as uds rather than the meson-baryon component, $\Lambda(1405)$ would have finite spatial size coming from the quark dynamics. This would lead to the additional contribution to the decay width, and hence the decay width in Fig. 4 would be shifted upward. Nevertheless, in this study we do not take into account such a contribution since a usual constituent quark model cannot describe $\Lambda(1405)$, which indicates that the ordinary quark configuration inside $\Lambda(1405)$ is small.

We also note that our relation would be model dependent mainly from the formulation of the radiative decay widths. Actually we might include form factors for the meson-baryon-baryon couplings, or we might use a usual Dirac-field propagators for baryons. These effects altogether would lead to $\sim$10% errors. Nevertheless, the scenario that the larger radiative decay width to $\Lambda\gamma$ directly leads to the larger absolute value of the $\bar{K}N$ compositeness would not be changed.

C. Analysis from the Λ(1405) pole position

In the previous subsection we have obtained the relation between the $\Lambda(1405)$ radiative decay width and the absolute value of the $\bar{K}N$ compositeness with the $\Lambda(1405)$ pole position determined from the value by the Particle Data Group. However, as we have already mentioned, the $\Lambda(1405)$ pole position is not well determined in experiments, and moreover $\Lambda(1405)$ has two poles according to the chiral unitary approach. Therefore, in this subsection we analyze how our relation between the radiative decay width and the absolute value of the $\bar{K}N$ compositeness $|X_{\bar{K}N}|$ depends on the $\Lambda(1405)$ pole position.

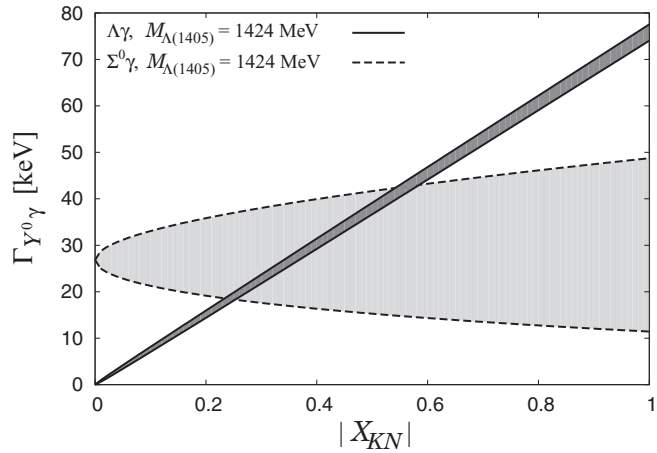

FIG. 5. Radiative decay width of $\Lambda(1405)$ as a function of the absolute value of the $\bar{K}N$ compositeness. The $\Lambda(1405)$ mass is fixed as $M_{\Lambda(1405)} = 1424$ MeV.

First we show how the relation shown in Fig. 4 is changed when the $\Lambda(1405)$ mass, i.e., the real part of the pole position, shifts upward to $M_{\Lambda(1405)} = 1424$ MeV, as the higher $\Lambda(1405)$ pole in the chiral unitary approach. In this condition, nevertheless, we expect that the relation shown in Fig. 4 will be not largely changed because we have shown that for the $\bar{K}N$ bound state the binding energy dependence of the relation between the $\bar{K}N$ compositeness and the radiative decay width is very small (see Fig. 3). Indeed, by using $M_{\Lambda(1405)} = 1424$ MeV instead of $M_{\Lambda(1405)} = 1405$ MeV, we obtain the relation between the absolute value of the $\bar{K}N$ compositeness and the radiative decay width shown in Fig. 5. The result with $M_{\Lambda(1405)} = 1424$ MeV is similar to that with $M_{\Lambda(1405)} = 1405$ MeV shown in Fig. 4 but the decay widths are slightly larger according to the larger $\Lambda(1405)$ mass. Then, by using the relation in Fig. 5 we could estimate the absolute value of the $\bar{K}N$ compositeness from the "experimental" value [27]: $|X_{\bar{K}N}| = 0.4^{+0.1}_{-0.2}$ from $\Gamma_{\Lambda\gamma} = 27 \pm 8$ keV, $|X_{\bar{K}N}| > 0.6$ from $\Gamma_{\Sigma^0\gamma} = 10 \pm 4$ keV, while $|X_{\bar{K}N}|$ can have an arbitrary value witnin $\Gamma_{\Sigma^0\gamma} = 23 \pm 7$ keV. These results, especially from $\Gamma_{\Lambda\gamma}$, would indicate that the absolute value of the $\bar{K}N$ compositeness inside $\Lambda(1405)$ would decrease slightly when a larger $\Lambda(1405)$ mass is used.

However, we should emphasize that the "experimental" value in Ref. [27] is extracted from an isobar model fitting of the decays of the K^-p atom with the assumption $M_{\Lambda(1405)} = 1405$ MeV. Besides, in the chiral unitary approach the $K^-p \to$ meson-baryon scatterings around and below the K^-p threshold contains more weight on the higher $\Lambda(1405)$ pole of the mass $\sim$1420 MeV, which is indeed supported by the $K^-d \to \pi\Sigma n$ reaction [47–51] and also by the absorption branching

ratios of K^- from an atomic orbit [60]. Therefore, it is better to make a simple reanalysis of the data on the branching ratios $\Gamma_{K^-p\to\Lambda\gamma}/\Gamma_{K^-p\to\text{anything}}$ and $\Gamma_{K^-p\to\Sigma^0\gamma}/\Gamma_{K^-p\to\text{anything}}$ used in Ref. [27] with the mass and the coupling constant g_{K^-p} for the higher $\Lambda(1405)$ pole listed in Table II. Actually, by replacing the parameters $M_{\Lambda(1405)} = 1405$ MeV and $g_{K^-p} = 3.2$ used in Ref. [27] with $M_{\Lambda(1405)} = 1424$ MeV and $g_{K^-p} = 2.25 + 0.87i$, we have obtained the larger radiative decay widths $\Gamma_{\Lambda\gamma} = 38 \pm 8$ keV and $\Gamma_{\Sigma^0\gamma} = 17 \pm 5$ or 42 ± 7 keV mainly due to the larger $\Lambda(1405)$ mass. Then, combined with the relation in Fig. 5, these values produce the absolute value of the $\bar{K}N$ compositeness as $|X_{\bar{K}N}| = 0.5 \pm 0.1$ from $\Gamma_{\Lambda\gamma} = 38 \pm 8$ keV, $|X_{\bar{K}N}| > 0.1$ from $\Gamma_{\Sigma^0\gamma} = 17 \pm 5$ keV, and $|X_{\bar{K}N}| > 0.2$ from $\Gamma_{\Sigma^0\gamma} = 42 \pm 7$ keV. From this estimation, we can see that the result of the absolute value of the $\bar{K}N$ compositeness from the $\Lambda\gamma$ decay is consistent with that in the previous subsection using $M_{\Lambda(1405)} = 1405$ MeV throughout the analysis. This means that our main conclusion of the absolute value of the $\bar{K}N$ compositeness from the K^-p atom data will not be changed even if the $\Lambda(1405)$ pole position is not well determined. We note that in order to reduce the ambiguity coming from analysis of the experimental data, it is necessary to determine the $\Lambda(1405)$ radiative decay width in a model-independent way.

Next, in the two-pole scenario for $\Lambda(1405)$, the reaction process controls which resonance pole has more weight. Actually the $\bar{K}N \to \pi\Sigma$ reaction process gives more weight to the higher resonance pole around 1420 MeV while $\pi\Sigma \to \pi\Sigma$ gives more weight to the lower pole [8]. For instance, in Ref. [36] the authors observe different shapes for the $\Lambda\gamma$ and $\Sigma^0\gamma$ invariant mass distributions in the $K^-p \to \pi^0 Y^0\gamma$ and $\pi^-p \to K^0 Y^0\gamma$ reactions, according to the different weights to the two $\Lambda(1405)$ poles. Namely, the former (latter) reaction is dominated by the higher (lower) $\Lambda(1405)$ pole. In the above discussion on the radiative decay we have considered the higher pole contribution. Then, it is useful to discuss how the $\bar{K}N$ compositeness can be observed with the dominance of the lower pole contribution such as in the $\pi^-p \to K^0\Lambda\gamma$ reaction. Here we show in Fig. 6 the relation between the absolute value of the $\bar{K}N$ compositeness inside the lower $\Lambda(1405)$ and its radiative decay width with the $\Lambda(1405)$ mass $M_{\Lambda(1405)} = 1381$ MeV and the $\pi^\pm\Sigma^\mp$ coupling constants listed in Table II. As one can see, the branching ratios of the $\Lambda\gamma$ and $\Sigma^0\gamma$ decay modes are different from the previous cases; as a reflection of the lower pole structure, the $\Sigma^0\gamma$ is dominant in the radiative decay even when $|X_{\bar{K}N}|$ is close to unity. We also observe a wider band both for the $\Lambda\gamma$ and $\Sigma^0\gamma$ decay modes, which originates from the larger $\pi\Sigma$ coupling constant $g_{\pi\Sigma}$. Nevertheless, the mean value of the allowed range for the $\Lambda\gamma$ decay shows behavior very similar to that in Fig. 4, which means that we can extract similar absolute value of the $\bar{K}N$ compositeness with a certain value of $\Gamma_{\Lambda\gamma}$ from both allowed regions of the $\Lambda\gamma$ mode in Figs. 4 and 6. From this analysis, it is interesting to observe the $\Lambda(1405)$ radiative decay in different $\Lambda(1405)$ production reactions, in which we might observe the different branching ratios of the radiative decay as evidence of the two-pole structure for $\Lambda(1405)$ and also the different $\bar{K}N$ compositeness for $\Lambda(1405)$.

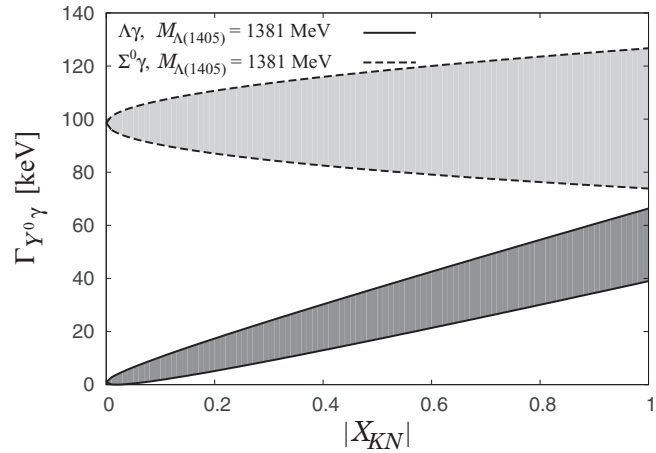

FIG. 6. Radiative decay width of $\Lambda(1405)$ as a function of the absolute value of the $\bar{K}N$ compositeness. The $\Lambda(1405)$ mass is fixed as $M_{\Lambda(1405)} = 1381$ MeV and the $\pi^\pm\Sigma^\mp$ coupling constants in Table II are used.

V. CONCLUSION

In this study we have investigated the radiative decay of $\Lambda(1405)$, $\Lambda(1405) \to \Lambda\gamma$ and $\Sigma^0\gamma$, from the viewpoint of the $\bar{K}N$ compositeness, which measures the amount of the $\bar{K}N$ component inside $\Lambda(1405)$. Since we can evaluate the $\bar{K}N$ compositeness by using the $\Lambda(1405)$-$\bar{K}N$ coupling constant and the $\Lambda(1405)$ pole position, we can establish a relation between the radiative decay width and the $\bar{K}N$ compositeness by expressing the radiative decay width with the $\bar{K}N$ coupling constant.

In order to grasp the behavior of the radiative decay width as a function of the $\bar{K}N$ compositeness, we first consider a $\bar{K}N(I = 0)$ bound state without couplings to other channels. Since there are one-to-one correspondences between the coupling constant of the bound state to $\bar{K}N$ and the $\bar{K}N$ compositeness as well as the bound state–$\bar{K}N$ coupling constant and the radiative decay width, we have established a relation between the $\bar{K}N$ compositeness and the radiative decay width. Especially the radiative decay width of the bound state is proportional to the compositeness, since both the radiative decay width and the compositeness are proportional to the squared bound state–$\bar{K}N$ coupling constant. We have obtained that the decay to $\Sigma^0\gamma$ is suppressed compared to the decay to $\Lambda\gamma$ due to the strengths of the $K^-p\Lambda$ and $K^-p\Sigma^0$ couplings. Furthermore, we have found that the binding energy dependence of the relation between the $\bar{K}N$ compositeness and the radiative decay width is very small.

Bearing in mind the discussions on the radiative decay width of the bound state, we have investigated the radiative decay of $\Lambda(1405)$. Here the absolute value of the $\Lambda(1405)$-$\bar{K}N$ coupling constant is determined from the absolute value of the $\bar{K}N$ compositeness, while the $\Lambda(1405)$-$\pi\Sigma$ coupling constant is estimated from the strong decay of $\Lambda(1405) \to \pi\Sigma$. In order to take into account the interference between $\bar{K}N$ and $\pi\Sigma$ in the decay amplitude, we calculate the maximally constructive and destructive interference, and we have shown the allowed region of the radiative decay width of $\Lambda(1405)$ as a function of

the absolute value of the $\bar{K}N$ compositeness. We note that the absolute value of the $\bar{K}N$ compositeness cannot be interpreted as a probability of finding the $\bar{K}N$ component but it will be an important piece of information on the structure of $\Lambda(1405)$. From the result of the radiative decay width we have found that the allowed region for the decay to $\Lambda\gamma$ is very narrow while that for the decay to $\Sigma^0\gamma$ is broad, since the decay to $\Lambda\gamma$ ($\Sigma^0\gamma$) is dominated by the $\bar{K}N$ ($\pi\Sigma$) component inside $\Lambda(1405)$. This means that the decay to $\Lambda\gamma$ is suited to study the $\bar{K}N$ component in $\Lambda(1405)$. Furthermore, by using the "experimental" data on the radiative decay width the absolute value of the $\bar{K}N$ compositeness is estimated as $|X_{\bar{K}N}| \gtrsim 0.5$, which implies that $\bar{K}N$ seems to be the largest component inside $\Lambda(1405)$. We have also discussed the pole position dependence of the radiative decay width, and have found that our main conclusion of the absolute value of the $\bar{K}N$ compositeness from the $K^- p$ atom data will not be changed even when the $\Lambda(1405)$ pole position is not well determined. On the other hand, in the two-pole scenario for $\Lambda(1405)$, we would observe the different branching ratios of the radiative decay and the different $\bar{K}N$ compositeness for $\Lambda(1405)$ in different $\Lambda(1405)$ production reactions, which could be evidence of the two-pole structure for $\Lambda(1405)$. Finally we emphasize that, in order to evaluate more precisely the $\bar{K}N$ compositeness of $\Lambda(1405)$ from experiments, it is necessary to determine precisely the radiative decay width of $\Lambda(1405)$ in various production reactions in a model-independent way.

ACKNOWLEDGMENT

This work was partially supported by the MEXT KAKENHI Grant No. 25105010.

APPENDIX A: FEYNMAN RULES

In this Appendix we summarize the Feynman rules used in this study.

In this study we use the propagators

$$P_m(p^2) = \frac{i}{p^2 - m^2 + i\epsilon}, \quad P_M(p^2) = \frac{2iM}{p^2 - M^2 + i\epsilon}, \tag{A1}$$

for mesons and baryons, respectively, where p is the momentum, m and M are the masses of the propagating meson and baryon, respectively, and ϵ is an infinitesimal positive value. The Dirac matrices in P_M are suppressed by an assumption that baryons go almost on-shell.

Due to the requirement of gauge invariance, the elementary couplings of the photon to the mesons and baryons should be given by the minimal coupling. As a result, the γMM and γBB vertices are given as

$$\begin{aligned} -iV_{\gamma MM} &= -ieQ_M\epsilon_\mu(p+p')^\mu, \\ -iV_{\gamma BB} &= -ieQ_B\epsilon_\mu\frac{(p+p')^\mu}{2M}, \end{aligned} \tag{A2}$$

with the elementary charge e, the charges of meson and baryon, Q_M and Q_B, respectively, the photon polarization ϵ_μ, and the incoming and outgoing momenta for the hadrons p^μ and p'^μ, respectively. Although the magnetic moments of the baryons could contribute to the γBB vertex, they are small and the contribution vanishes in the heavy baryon limit in this study as discussed in Ref. [36].

The MBB coupling can be obtained from the lowest-order SU(3) chiral Lagrangian,

$$\mathcal{L} = -\frac{D+F}{\sqrt{2}f}\mathrm{tr}[\bar{B}\gamma^\mu\gamma_5\partial_\mu\Phi B] - \frac{D-F}{\sqrt{2}f}\mathrm{tr}[\bar{B}\gamma^\mu\gamma_5 B\partial_\mu\Phi], \tag{A3}$$

with the meson decay constant f, parameters D and F, and the flavor SU(3) matrices for the baryons B and Nambu-Goldstone bosons Φ. This Lagrangian generates the MBB vertex as

$$-iV_{MBB} = -\tilde{V}_{MBB}\gamma^\mu\gamma_5 q_\mu, \tag{A4}$$

$$\tilde{V}_{MBB} \equiv \alpha_{MBB}\frac{D+F}{2f} + \beta_{MBB}\frac{D-F}{2f}, \tag{A5}$$

with the incoming meson momentum q^μ. Then the nonrelativistic reduction $\gamma^\mu\gamma_5 q_\mu \to -\boldsymbol{\sigma}\cdot\boldsymbol{q}$ leads the vertex to

$$-iV_{MBB} = \tilde{V}_{MBB}\boldsymbol{\sigma}\cdot\boldsymbol{q} = -\tilde{V}_{MBB}\sigma_\mu q^\mu, \tag{A6}$$

with $\sigma^\mu = (0, \boldsymbol{\sigma})$.

Finally the γMBB vertex is obtained by applying the minimal coupling with respect to the MBB coupling as

$$-iV_{\gamma MBB} = -eQ_M\boldsymbol{\epsilon}\cdot\boldsymbol{\sigma}\tilde{V}_{MBB} = eQ_M\epsilon_\mu\sigma^\mu\tilde{V}_{MBB} \tag{A7}$$

where the nonrelativistic reduction has been used.

APPENDIX B: WARD IDENTITY FOR THE RADIATIVE DECAY AMPLITUDE

In this Appendix we prove the Ward identity for the radiative decay amplitude used in this study. Here we consider a general case with nonzero total charge $Q_T = Q_M + Q_B \neq 0$, which is not the case of the $\Lambda(1405)$ radiative decay, but consider only the single channel. Due to the nonzero total charge, we have diagrams for the radiative decay shown in Fig. 7 in addition to those in Fig. 2. By using the Feynman rules and the condition $k^2 = 0$, their decay amplitudes can be expressed as

$$-iT_{(d)} = +egQ_T\tilde{V}\sigma_\mu\epsilon_\nu^*\frac{(2P-k)^\nu}{2P\cdot k}L^\mu(P), \tag{B1}$$

$$-iT_{(e)} = -egQ_T\tilde{V}\sigma_\mu\epsilon_\nu^*\frac{(2P-k)^\nu}{2P\cdot k}L^\mu(P-k), \tag{B2}$$

where the loop integral $L^\mu(P)$ is defined as

$$L^\mu(P) \equiv i\int\frac{d^4q}{(2\pi)^4}\frac{q^\mu}{q^2-m^2}\frac{1}{(P-q)^2-M^2}. \tag{B3}$$

The other three amplitudes are given in Eqs. (12), (13), and (14).

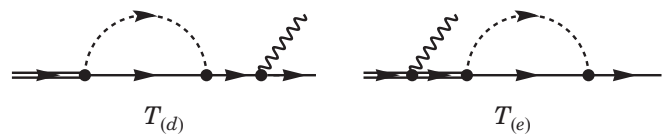

FIG. 7. Supplemental Feynman diagrams for the radiative decay with nonzero total charge.

The Ward identity states that sum of the five amplitudes becomes zero if one takes $\epsilon_\nu^* \to k_\nu$ for on-shell photon, $k^2 = 0$. In order to prove this, we first show the relations for $k_\nu D_1^{\mu\nu}$ and $k_\nu D_2^{\mu\nu}$,

$$k_\nu D_1^{\mu\nu} = L^\mu(P-k) - L^\mu(q) + k^\mu G(P), \tag{B4}$$

$$k_\nu D_2^{\mu\nu} = L^\mu(P-k) - L^\mu(q), \tag{B5}$$

which can be obtained by using the identity

$$\frac{k_\nu(2q-k)^\nu}{[(q-k)^2-m^2][q^2-m^2]} = \frac{1}{(q-k)^2-m^2} - \frac{1}{q^2-m^2}, \tag{B6}$$

with $k^2 = 0$. Then, with the replacement of $\epsilon_\nu^* \to k_\nu$, the decay amplitudes become

$$T_{(a)} \to -ieg Q_M \tilde{V}\sigma_\mu k^\mu G(P), \tag{B7}$$

$$T_{(b)} \to +ieg Q_M \tilde{V}\sigma_\mu [L^\mu(P-k) - L^\mu(P) + k^\mu G(P)], \tag{B8}$$

$$T_{(c)} \to +ieg Q_B \tilde{V}\sigma_\mu [L^\mu(P-k) - L^\mu(P)], \tag{B9}$$

$$T_{(d)} \to +ieg Q_T \tilde{V}\sigma_\mu L^\mu(P), \tag{B10}$$

$$T_{(e)} \to -ieg Q_T \tilde{V}\sigma_\mu L^\mu(P-k), \tag{B11}$$

As a result, we obtain

$$T_{(a)} + T_{(b)} + T_{(c)} + T_{(d)} + T_{(e)} \to 0. \tag{B12}$$

for $\epsilon_\nu^* \to k_\nu$. This means that the Ward identity is indeed satisfied for the five amplitudes. Here we have assumed the decay in the single channel, but Eq. (B12) indicates that the Ward identity is satisfied in each channel. This is reasonable, because in the multichannel approach we may take the coupling constant g_i independently for each channel i, and hence the Ward identity should be satisfied independently in each channel. Finally we emphasize that if $Q_T = 0$, as is the case of the $\Lambda(1405)$ radiative decay, we do not have $T_{(d)}$ and $T_{(e)}$ and hence the Ward identity is satisfied even for the three amplitudes $T_{(a)}$, $T_{(b)}$, and $T_{(c)}$.

[1] J. Beringer *et al.* (Particle Data Group Collaboration), Phys. Rev. D **86**, 010001 (2012).
[2] R. H. Dalitz and S. F. Tuan, Ann. Phys. (N.Y.) **10**, 307 (1960).
[3] R. H. Dalitz, T. C. Wong, and G. Rajasekaran, Phys. Rev. **153**, 1617 (1967).
[4] N. Kaiser, P. B. Siegel, and W. Weise, Nucl. Phys. A **594**, 325 (1995).
[5] E. Oset and A. Ramos, Nucl. Phys. A **635**, 99 (1998).
[6] J. A. Oller and U. G. Meissner, Phys. Lett. B **500**, 263 (2001).
[7] M. F. M. Lutz and E. E. Kolomeitsev, Nucl. Phys. A **700**, 193 (2002).
[8] D. Jido, J. A. Oller, E. Oset, A. Ramos, and U. G. Meissner, Nucl. Phys. A **725**, 181 (2003).
[9] M. Niiyama, H. Fujimura, D. S. Ahn, J. K. Ahn, S. Ajimura, H. C. Bhang, T. H. Chang, and W. C. Chang *et al.*, Phys. Rev. C **78**, 035202 (2008).
[10] K. Moriya *et al.* (CLAS Collaboration), Phys. Rev. C **87**, 035206 (2013).
[11] J. C. Nacher, E. Oset, H. Toki, and A. Ramos, Phys. Lett. B **455**, 55 (1999).
[12] S. Cho *et al.* (ExHIC Collaboration), Phys. Rev. Lett. **106**, 212001 (2011).
[13] S. Cho *et al.* (ExHIC Collaboration), Phys. Rev. C **84**, 064910 (2011).
[14] H. Kawamura, S. Kumano, and T. Sekihara, Phys. Rev. D **88**, 034010 (2013).
[15] T. Hyodo, D. Jido, and A. Hosaka, Phys. Rev. C **85**, 015201 (2012).
[16] F. Aceti and E. Oset, Phys. Rev. D **86**, 014012 (2012).
[17] C. W. Xiao, F. Aceti, and M. Bayar, Eur. Phys. J. A **49**, 22 (2013).
[18] F. Aceti, L. R. Dai, L. S. Geng, E. Oset, and Y. Zhang, arXiv:1301.2554.
[19] T. Hyodo, Int. J. Mod. Phys. A **28**, 1330045 (2013).
[20] A. Salam, Nuovo Cimento **25**, 224 (1962).
[21] S. Weinberg, Phys. Rev. **130**, 776 (1963).
[22] H. Ezawa, T. Muta, and H. Umezawa, Prog. Theor. Phys. **29**, 877 (1963).
[23] S. Weinberg, Phys. Rev. **137**, B672 (1965).
[24] V. Baru, J. Haidenbauer, C. Hanhart, Y. Kalashnikova and A. E. Kudryavtsev, Phys. Lett. B **586**, 53 (2004).
[25] C. Hanhart, Eur. Phys. J. A **35**, 271 (2008).
[26] C. Hanhart, Y. S. Kalashnikova, and A. V. Nefediev, Eur. Phys. J. A **47**, 101 (2011).
[27] H. Burkhardt and J. Lowe, Phys. Rev. C **44**, 607 (1991).
[28] J. W. Darewych, M. Horbatsch, and R. Koniuk, Phys. Rev. D **28**, 1125 (1983).
[29] E. Kaxiras, E. J. Moniz, and M. Soyeur, Phys. Rev. D **32**, 695 (1985).
[30] M. Warns, W. Pfeil, and H. Rollnik, Phys. Lett. B **258**, 431 (1991).
[31] Y. Umino and F. Myhrer, Nucl. Phys. A **554**, 593 (1993).
[32] C. L. Schat, N. N. Scoccola, and C. Gobbi, Nucl. Phys. A **585**, 627 (1995).
[33] R. Bijker, F. Iachello, and A. Leviatan, Ann. Phys. (N.Y.) **284**, 89 (2000).
[34] T. Van Cauteren, J. Ryckebusch, B. Metsch, and H.-R. Petry, Eur. Phys. J. A **26**, 339 (2005).
[35] L. Yu, X.-L. Chen, W.-Z. Deng, and S.-L. Zhu, Phys. Rev. D **73**, 114001 (2006).
[36] L. S. Geng, E. Oset, and M. Doring, Eur. Phys. J. A **32**, 201 (2007).
[37] C. S. An, B. Saghai, S. G. Yuan, and J. He, Phys. Rev. C **81**, 045203 (2010).
[38] M. Doring, D. Jido, and E. Oset, Eur. Phys. J. A **45**, 319 (2010).
[39] T. Hyodo, D. Jido, and A. Hosaka, Phys. Rev. C **78**, 025203 (2008).
[40] T. Hyodo, D. Jido, and L. Roca, Phys. Rev. D **77**, 056010 (2008).
[41] L. Roca, T. Hyodo, and D. Jido, Nucl. Phys. A **809**, 65 (2008).
[42] T. Sekihara, T. Hyodo, and D. Jido, Phys. Lett. B **669**, 133 (2008).
[43] T. Sekihara, T. Hyodo, and D. Jido, Phys. Rev. C **83**, 055202 (2011).
[44] T. Sekihara and T. Hyodo, Phys. Rev. C **87**, 045202 (2013).
[45] T. Hyodo and D. Jido, Prog. Part. Nucl. Phys. **67**, 55 (2012).
[46] T. Hyodo and W. Weise, Phys. Rev. C **77**, 035204 (2008).

[47] O. Braun, H. J. Grimm, V. Hepp, H. Strobele, C. Thol, T. J. Thouw, D. Capps and F. Gandini *et al*., Nucl. Phys. B **129**, 1 (1977).
[48] D. Jido, E. Oset, and T. Sekihara, Eur. Phys. J. A **42**, 257 (2009).
[49] D. Jido, E. Oset, and T. Sekihara, Eur. Phys. J. A **47**, 42 (2011).
[50] J. Yamagata-Sekihara, T. Sekihara, and D. Jido, Prog. Theor. Exp. Phys. **2013**, 043D02.
[51] D. Jido, E. Oset, and T. Sekihara, Eur. Phys. J. A **49**, 95 (2013).
[52] H. Y. Lu *et al*. (CLAS Collaboration), Phys. Rev. C **88**, 045202 (2013).
[53] M. Doring, Nucl. Phys. A **786**, 164 (2007).
[54] F. E. Close, N. Isgur, and S. Kumano, Nucl. Phys. B **389**, 513 (1993).
[55] J. A. Oller, Phys. Lett. B **426**, 7 (1998).
[56] E. Marco, S. Hirenzaki, E. Oset, and H. Toki, Phys. Lett. B **470**, 20 (1999).
[57] L. Roca, A. Hosaka, and E. Oset, Phys. Lett. B **658**, 17 (2007).
[58] Y. Ikeda, T. Hyodo, and W. Weise, Phys. Lett. B **706**, 63 (2011).
[59] Y. Ikeda, T. Hyodo, and W. Weise, Nucl. Phys. A **881**, 98 (2012).
[60] T. Sekihara, J. Yamagata-Sekihara, D. Jido, and Y. Kanada-En'yo, Phys. Rev. C **86**, 065205 (2012).